

# Extracting statistical distributions of RTN originating from both acceptor-like and donor-like traps

Kean H. Tok, Jian F. Zhang, James Brown, Zhigang Ji\*, and Weidong Zhang

School of Engineering, Liverpool John Moores University,  
Byrom Street, Liverpool L3 3AF, UK

\*Also at School of Microelectronics, Shanghai Jiaotong University, Shanghai 200240, P. R. China  
Email: j.f.zhang@ljmu.ac.uk

## Abstract

The impact of Random Telegraph Noise (RTN) on devices increases, as the device sizes are downscaled. Against a reference level, it is commonly observed that RTN can fluctuate both below and above this level. The modelling of RTN, however, was typically carried out only in the direction where drain current reduces. In reality, this current reduction can be compensated by simultaneous current increases. This calls the accuracy of the one-directional RTN modelling into questions. Separating the fluctuation in one direction from the other is difficult experimentally. In this paper, we review the recently proposed integral methodology for achieving this separation. In contrast with early works, the integral methodology does not require selecting devices with fluctuation only in one direction. The RTN in all devices are measured and grouped together to form one dataset. It is then statically analyzed by assuming the presence of fluctuation in both directions. In this way, the separation is carried out numerically, rather than experimentally. Based on the maximum likelihood estimation, the popular statistical distributions are tested against experimental data. It is found that the General Extreme Value (GEV) distribution agrees best with the experimental threshold voltage shift, when compared with the Exponential and Lognormal distributions.

## 1. Introduction

As devices downscale, they increasingly suffer from Random Telegraph Noise (RTN) [1-11], in addition to ageing [12-18]. When there is only one trap in gate dielectric, Fig. 1(a) shows it can capture and then emit a charge carrier, resulting in RTN in Fig. 1(b). For a nMOSFET, early works [1-7] focused on acceptor-like traps in gate dielectric, which capture electrons, become negatively charged, and leads to a reduction of drain current,  $I_d$ . Similarly, for a pMOSFET, attentions were focused on donor-like traps, which capture holes, become positively charged, and result in a reduction of the magnitude of  $I_d$ . The fluctuation in  $I_d$  was typically measured as  $\Delta I_d/I_d$ , where  $\Delta I_d$  can be defined as,

$$\Delta I_d = I_{d,ref} - I_d. \quad (1)$$

The  $I_{d,ref}$  is typically measured from the average of the first several points before the traps become electrically active and the RTN transition starts, as shown by the blue line in Fig. 2. By the definition in Eq.(1), a positive  $\Delta I_d/I_d$  represents a reduction of  $I_d$  after filling a trap. Early works [1-7] focused on modelling  $\Delta I_d/I_d > 0$ . When  $I_d$  was monitored against time under constant  $V_g$  and  $V_d$ , however,  $\Delta I_d/I_d$  can be either positive or negative and one example is given in Fig. 2. Fig. 3 shows that there is little correlation between the positive and negative  $\Delta I_d/I_d$ , so that the model developed for one cannot be used for the other. For a RTN model to be applicable to generic devices, it must cover both  $\Delta I_d/I_d > 0$  and  $\Delta I_d/I_d < 0$ . The aim of this work is to review the recent proposed integral methodology that models  $\Delta I_d/I_d$  in both directions.

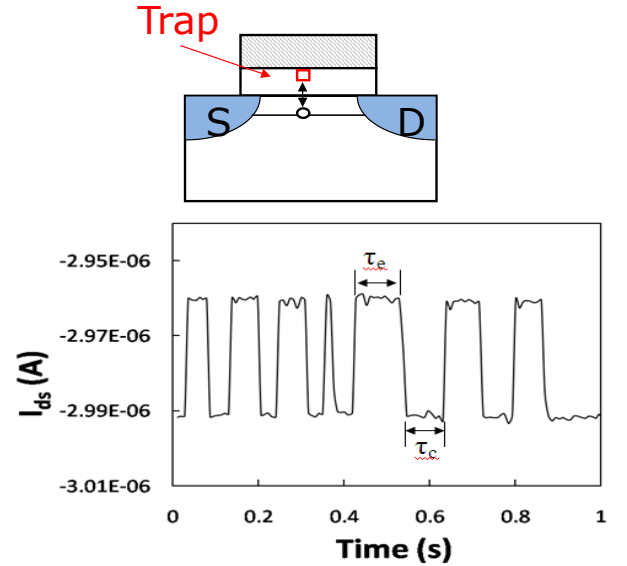


Fig. 1. (a) An schematic illustration of capturing and emitting charge carrier by a trap in gate dielectric. (b) A typical two level RTN.

## 2. Methodology

For a nMOSFET, it is generally agreed that  $\Delta I_d/I_d > 0$  originates from acceptor-like electron traps, which

capture electrons from the channel, form negative charges in gate dielectric, and reduce  $I_d$ . There are different interpretations for  $\Delta I_d/I_d < 0$ . One of them is that they originate from donor-like hole traps, which form positive charges and increase  $I_d$ . The other is that, when  $I_{d,ref}$  was measured, some acceptor-like traps were already filled with electrons. These traps then emit electrons, resulting in the observed  $\Delta I_d/I_d < 0$ . Our test results do not conclude which interpretation is correct. For the convenience of presentation, we will use the terms of acceptor-like and donor-like traps, thereafter.

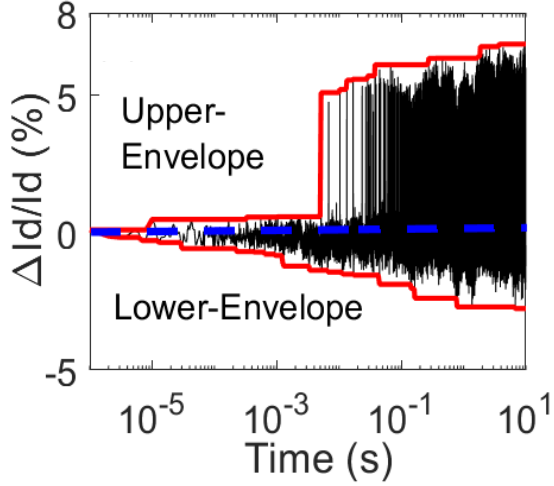


Fig. 2. Raw data of the measured RTN (Black lines). The envelopes are represented by the red lines. [19].

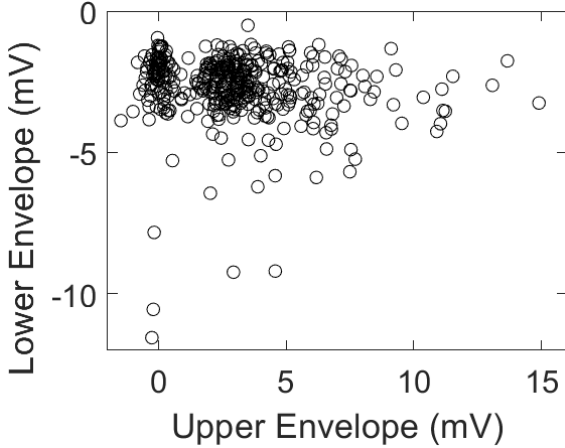


Fig. 3. The lower envelope has little correlation with the upper-envelope. [19].

The RTN can cause fluctuation in both  $I_d$  and threshold voltage,  $V_{th}$ . Early works [4,5,11] often converted  $\Delta I_d$  to  $\Delta V_{th}$  by,

$$\Delta V_{th} = \frac{\Delta I_d}{g_m}, \quad (2)$$

where  $g_m$  is the transconductance. When compared with the  $\Delta V_{th}$  directly measured from the pulse  $I_d$ - $V_g$  at  $V_g = V_{th}$ , Fig. 4 shows that the Eq. (2) is accurate only when the  $V_g$  is close to  $V_{th}$ . To simplify the test procedure and to minimize the inaccuracy, the  $\Delta I_d$  will be measured at  $V_g = 0.5$  V, which is sufficiently close to  $V_{th} = 0.45$  V that the Eq. (2) is applicable. The  $g_m$  was measured for each device from a pulse  $I_d$ - $V_g$  before starting the RTN test. We will present our model in terms of  $\Delta V_{th}$ , hereafter.

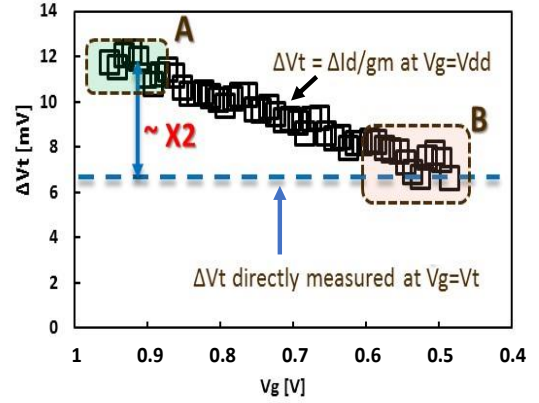


Fig. 4. A comparison of the  $\Delta V_{th}$  evaluated from  $\Delta I_d/g_m$  at different  $V_g$  with the  $\Delta V_{th}$  measured at  $V_g = V_{th}$ .

There are theoretical and experimental difficulties for modelling both  $\Delta I_d/I_d > 0$  and  $\Delta I_d/I_d < 0$  simultaneously. Theoretically, the well-known statistical distributions, such as Exponential and Lognormal distributions, require  $\Delta V_{th}$  to be positive only [19], which corresponds to charging acceptor-like electron traps in nMOSFETs. In order to model both positive and negative  $\Delta V_{th}$ , we will use two statistical distributions: one for the positive  $\Delta V_{th_A}$  and the other for the magnitude of the negative  $\Delta V_{th_D}$ ,  $|\Delta V_{th_D}|$ , where the subscript 'A' and 'D' represents acceptor-like and donor-like traps, respectively. The total  $\Delta V_{th}$  can then be evaluated from,

$$\Delta V_{th} = \Delta V_{th_A} + \Delta V_{th_D}, \quad (3)$$

Experimentally, one can only measure the combined effect of acceptor-like and donor-like traps. As they compensate each other, the measured  $\Delta V_{th}$  cannot be attributed to one type of traps. As a result, it is difficult to separate these two types of traps experimentally.

To overcome the above challenges, an integral methodology has been developed which does not require separating acceptor-like from donor-like traps experimentally [19,20]. Instead, the  $\Delta V_{th}$  measured from each device will be grouped together to form a data set. At a given time, one  $\Delta V_{th} = \Delta I_d/g_m$  is taken for each device from the raw measured data like those shown in Fig. 2. By repeating the measurement on 402 devices, we have 402  $\Delta V_{th}$ , as shown in Fig. 5.

To model the cumulative distribution function (CDF) of  $\Delta V_{th}$  in Fig. 5, it is assumed that the number of both acceptor-like traps,  $N_A$ , and donor-like traps,  $N_D$ , per device follows the Poisson distribution. The impact of one trap on the device,  $\delta V_{th}$ , follows one of: Exponential, Lognormal, or General Extreme Value (GEV) distributions [2,7]. It should be pointed out that  $\delta V_{th}$  is the shift per traps, which is different from the shift per device  $\Delta V_{th}$ , as multiple traps can contribute to  $\Delta V_{th}$ . In addition, the thermal noise is also taken into account by using a normal distribution with zero average value. The parameters in these distributions will be extracted by the Maximum Likelihood Estimations. In this way, the measured  $\Delta V_{th}$  is separated into contribution of individual traps numerically and statistically, rather than experimentally.

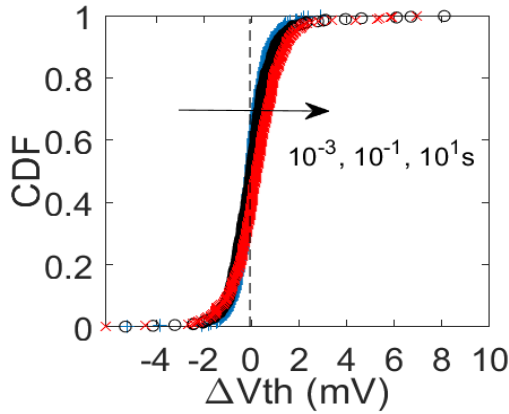


Fig. 5. A comparison of the CDF of  $\Delta V_{th}$  at different time. [19].

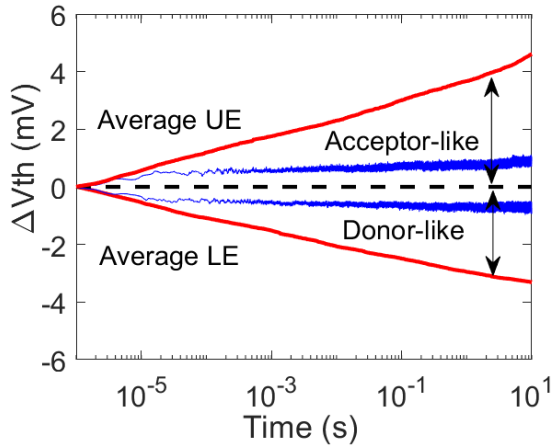


Fig. 6. A comparison of the average envelope with the average values of  $\Delta V_{th}>0$  and  $\Delta V_{th}<0$ . [19].

Early works [6,21-27] studied the envelopes of the RTN induced fluctuation in Fig.2. In this work, however, we model the  $\Delta V_{th}$  itself, rather than its envelope. For one device, Fig. 2 shows that  $\Delta V_{th}$  (black lines) at a given

time point can be substantially lower than its envelope. The upper-envelope in Fig. 2 represent the maximum  $\Delta V_{th_A}$  up to that time point, when acceptor-like traps are charged. Most of the time, however, some acceptor-like traps are neutral due to emission, so that most of measured  $\Delta V_{th}$  is below the envelope. In another word,  $\Delta V_{th}$  only hits its envelope occasionally, when there are multiple traps in a device. Similarly the lower envelop represents  $\Delta V_{th_D}$  when donor-like traps are charged.

To statistically compare the envelope with the average  $\Delta V_{th}$ , Fig. 6 plots the average envelopes measured on 402 devices with the average  $\Delta V_{th}>0$  and  $\Delta V_{th}<0$  of these devices. It can be seen that the average  $\Delta V_{th}>0$  is less than half of the average envelope. As a result, using the envelop will substantially overestimate RTN.

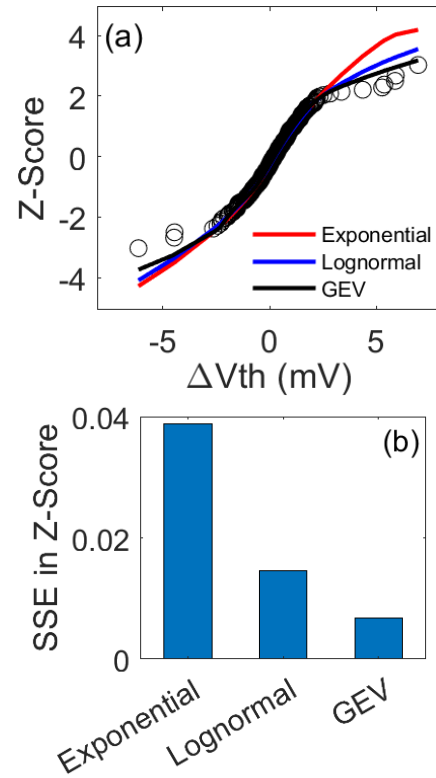


Fig. 7. (a) A comparison of the CDFs computed from the extracted distributions in Table I with the test data. (b) The Sum of Squared Errors of different distributions. [19].

### 3. Results

The parameters for different distributions were extracted based on the Maximum Likelihood Estimation and their values are given in Table I. Fig. 7(a) compares the CDF computed from these distributions with the experimental data. It can be seen that the GEV distribution agrees best with test data, while Exponential the worst. To enable a quantitative comparison, the sum of squared errors (SSE) per device is given in Fig. 7(b).

To explain why the GEV distribution agrees best with the measured  $\Delta V_{th}$ , it should be pointed out that GEV generally has longer distribution tails than the Exponential and Lognormal distributions. This makes it better suited to describe the widespread statistical events. Under  $V_g = V_{th}$ , the current flow follows percolation paths. The traps on top of these paths will have substantially larger impact than the traps away from them, giving a long distribution tail and matching the GEV distribution best.

Table I. Probability distribution functions (pdf) and their extracted parameter values. [19].

	PDF of $\delta V_{th}$	Acceptor	Donor
Exponential	$\frac{1}{\eta} e^{-\frac{\delta V_{th}}{\eta}}$	$\eta = 0.56$	$\eta = 0.48$
Lognormal	$\frac{1}{\delta V_{th} \theta \sqrt{2\pi}} e^{-\frac{(\ln(\delta V_{th}) - \epsilon)^2}{2\theta^2}}$	$\epsilon = -0.43$ $\theta = 0.12$	$\epsilon = -0.71$ $\theta = 0.16$
GEV	$\frac{1}{\beta} (k)^{\xi+1} e^{-k}$ $k = \left(1 + \xi \left(\frac{\delta V_{th} - \alpha}{\beta}\right)\right)^{-\frac{1}{\xi}}$	$\xi = 0.35$ $\alpha = 0.43$ $\beta = 0.34$	$\xi = 0.42$ $\alpha = 0.59$ $\beta = 0.19$
Thermal	$\frac{1}{\sigma\sqrt{2\pi}} e^{-\frac{1}{2}\left(\frac{\Delta V_{th}}{\sigma}\right)^2}$	<i>Exponential</i> , $\sigma = 0.11$ <i>Lognormal</i> , $\sigma = 0.13$ <i>GEV</i> , $\sigma = 0.13$	

#### 4. Conclusions

This work reviews the recently proposed integral methodology for modelling RTN. Early works only modeled RTN fluctuation in one direction and had to remove the devices with fluctuation in both directions. In contrast, the integral methodology does not select devices and can be used to model RTN fluctuation in both directions. It is assumed that both acceptor-like and donor-like traps exist simultaneously, which are responsible for positive and negative  $V_{th}$  shift, respectively. Instead of analyzing individual defects, the  $\Delta V_{th}$  measured on different devices are integrated together to form a dataset for statistical analysis. Based on the Maximum Likelihood Estimation, the parameters for different distributions have been extracted. It is found that the GEV distribution agrees best with the measured  $\Delta V_{th}$ .

#### Acknowledgments

The test samples were supplied by D. Vigar of CSR. This work is supported by EPSRC of UK under the grant no. EP/T026022/1.

#### References

[1] M. J. Kirton and M. J. Uren, *Advances in Physics*, 38, p.367 (1989).  
[2] R. Wang et al., *IEDM*, p.388 (2018).  
[3] M. Tanizawa et al, *VLSI Technol.*, p.95 (2010).  
[4] A. Manut, R. Gao, J. F. Zhang, Z. Ji, M. Mehedi, W.

D. Zhang, D. Vigar, A. Asenov, and B. Kaczer, *IEEE Trans. Elec. Dev.*, 66, p.1482 (2019).  
[5] T. Nagumo et al, *IEDM*, p.628, 2010.  
[6] M. Mehedi, K. H. Tok, J. F. Zhang, Z. Ji, Z. Ye, W. Zhang, and J. S. Marsland, *IEEE Access*, 8, p.1496 (2020).  
[7] M. Mehedi, K. H. Tok, Z. Ye, J. F. Zhang, Z. Ji, W. Zhang, and J. S. Marsland, *IEEE Access*, 9, p.43551 (2021).  
[8] J. Brown, R. Gao, Z. Ji, J. Chen, J. Wu, J. F. Zhang, B. Zhou, Q. Shi, J. Crawford, and W. Zhang, *VLSI Technol.*, p.95 (2018).  
[9] J. Brown, J. F. Zhang, B. Zhou, M. Mehedi, P. Freitas, J. S. Marsland and Z. Ji, *Scientific Reports*, 10, (2020).  
[10] Z. Chai et al., *IEEE Elec. Dev. Lett.*, 39, p.1652 (2018).  
[11] H. Miki et al., *VLSI Technol.*, p.137, (2012).  
[12] J. F. Zhang, Z. Ji, and W. Zhang, *Microelectronics Reliability*, 80, p.109 (2018).  
[13] Z. Ji, S. F. W. M. Hatta, J. F. Zhang, J. G. Ma, W. Zhang, N. Soin, B. Kaczer, S. De Gendt, and G. Groeseneken, *IEDM*, p.413 (2013).  
[14] R. Gao, Z. Ji, A. B. Manut, J. F. Zhang, J. Franco, S. W. M. Hatta, W. D. Zhang, B. Kaczer, D. Linten, and G. Groeseneken, *IEEE Trans. Elec. Dev.*, 64, p.4011 (2017).  
[15] R. Gao, A. B. Manut, Z. Ji, J. Ma, M. Duan, J. F. Zhang, J. Franco, S. W. M. Hatta, W. Zhang, B. Kaczer, D. Vigar, D. Linten, and G. Groeseneken, *IEEE Trans. Elec. Dev.*, 64, p.1467 (2017).  
[16] X. F. Zheng et al., *IEEE Trans. Elec. Dev.*, 57, p.288 (2009).  
[17] M. Duan, J. F. Zhang, Z. Ji, W. Zhang, B. Kaczer, S. De Gendt, and G. Groeseneken, *IEEE Elec. Dev. Lett.*, 33, p.480 (2012).  
[18] M. Duan, J. F. Zhang, Z. Ji, W. Zhang, D. Vigar, A. Asenov, L. Gerrer, V. Chandra, R. Aitken, and B. Kaczer, *IEEE Trans. Elec. Dev.*, 63, p. 3642 (2016).  
[19] K. H. Tok et al., *IEEE Trans. Elec. Dev.*, 69, p.3869 (2022).  
[20] K. H. Tok et al., *IEEE Trans. Elec. Dev.*, 69, p.5780 (2022).  
[21] M. Duan, et.al., *IEEE Trans. Electron Dev.*, 60, p.2505 (2013).  
[22] M. Duan, et.al., *IEEE Trans. Elec. Dev.*, 61, p.3081 (2014).  
[23] M. Duan, et.al., *IEDM*, p.547, 2015.  
[24] M. Duan, J. F. Zhang, Z. Ji, W. Zhang, B. Kaczer, and A. Asenov, *IEEE Trans. Elec. Dev.*, 64, p.2478 (2017).  
[25] M. Duan et al., *IEDM*, p. 774 (2013).  
[26] J. F. Zhang et al., *IEEE Elec. Dev. Lett.*, 27, p.817 (2006).  
[27] M. Duan et al., *IEEE Elec. Dev. Lett.*, 33, p.480 (2012).